Multimedia Environmental Distribution of Engineered Nanomaterials

ARTICLE *in* ENVIRONMENTAL SCIENCE & TECHNOLOGY · FEBRUARY 2014

Impact Factor: 5.33 · DOI: 10.1021/es405132z · Source: PubMed

2 AUTHORS:

Haoyang Haven Liu

10 PUBLICATIONS **115** CITATIONS

SEE PROFILE

Yoram Cohen

University of California, Los Angeles

262 PUBLICATIONS **5,943** CITATIONS

SEE PROFILE

Environmental Science & Technology

Article

pubs.acs.org/est

Multimedia Environmental Distribution of Engineered Nanomaterials

Haoyang Haven Liu[†,‡] and Yoram Cohen*[,†,‡]

[†]Center for the Environmental Implications of Nanotechnology, California Nanosystems Institute, University of California, Los Angeles, California 90095, United States

[‡]Chemical and Biomolecular Engineering Department, University of California, Los Angeles, Los Angeles, California 90095, United States

Supporting Information

ABSTRACT: A compartmental multimedia model was developed to enable evaluation of the dynamic environmental multimedia mass distribution and concentrations of engineered nanomaterials (ENMs). The approach considers the environment as a collection of compartments, linked via fundamental environmental intermedia transport processes. Model simulations for various environmental scenarios indicated that ENM accumulation in the sediment increased significantly with increased ENMs attachment to suspended solids in water. Atmospheric dry and wet depositions can be important pathways for ENMs input to the terrestrial environment in the absence of direct and distributed ENM release to soil. Increased ENM concentration in water due to atmospheric deposition (wet and dry) is expected as direct ENM release to water diminishes. However, for soluble ENMs dissolution can be the dominant pathway for suspended ENM removal from water even compared to advection. Mass accumulation in the multimedia environment for the evaluated ENMs (metal, metal oxides, carbon nanotubes (CNT), nanoclays) was mostly in the soil and sediment. The present modeling approach, as illustrated via different test cases, is suited for "what if" first tier analyses to assess the multimedia mass distribution of ENMs and associated potential exposure concentrations.

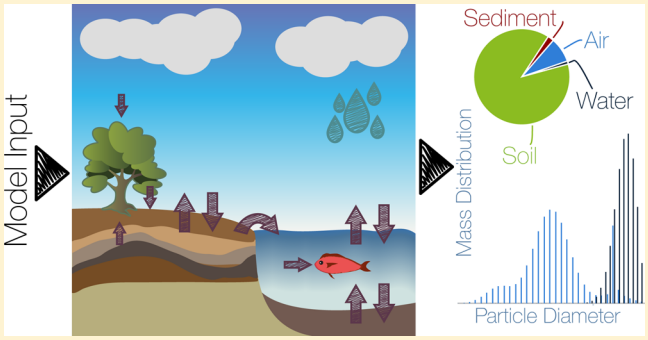

INTRODUCTION

Given rapid developments of new engineered nanomaterials (ENMs) and their increased utilization, there is a growing concern regarding potential adverse effects of ENMs on the environment and human health.[1−10] Consequently, efforts are mounting to assess potential releases, exposures, and toxicity of ENMs and their associated environmental impacts throughout their lifecycle.[11−17] ENMs that may be released to the environment (air emissions and/or direct discharge to surface water, etc.) are likely to move across environmental boundaries and thus will be found in most media.[18]

Field monitoring of the concentrations of ENMs would clearly be valuable for assessing the environmental multimedia distribution of ENMs. However, current technology for environmental detection and measurements of ENMs is still in the developing stage.[19−22] Even with the availability of advanced monitoring methods, deployment of a multimedia monitoring strategy would be a daunting and costly endeavor that may be impractical for the increasingly large number of ENMs. In this regard, estimation methods based on life-cycle assessment can inform decision makers as to potential environmental releases of ENMs during manufacturing, use, and product disposal.[23−27] Although there have been attempts to estimate ENMs media concentrations based on material flow analysis (MFA), such estimates are in general not based on fundamental multimedia fate and transport (F&T) analysis; thus, one is not assured of overall consistency and adherence to constraints that may be imposed by intermedia transport mechanisms.

Although potential environmental concentrations of pollutants can be estimated based on suitable multimedia F&T models, such models are yet to emerge for ENMs. Multimedia F&T models have been developed to assess the potential impact of chemical pollutants.[28−32] Such models have relied on mathematical constructs to describe the entry, movement, and distribution of chemicals within the environment,[29] in order to estimate their media concentrations and mass distributions. Multimedia analysis is typically a tiered process, which ranges from use of simple models consisting of well-mixed environmental compartments linked by intermedia transport processes[32] to complex single medium models at various levels of spatial resolution coupled (where feasible) with field monitoring.[32] First tier screening-level multimedia analysis[29] has been utilized for order-of-magnitude (or better) analysis of exposure concentrations and mass distribution of chemical pollutants in specific regions.[33−36] When warranted, higher tier models can be used for site-specific exposure analyses but often at the

Received: November 18, 2013
Revised: February 10, 2014
Accepted: February 18, 2014

   dx.doi.org/10.1021/es405132z | Environ. Sci. Technol. XXXX, XXX, XXX−XXX

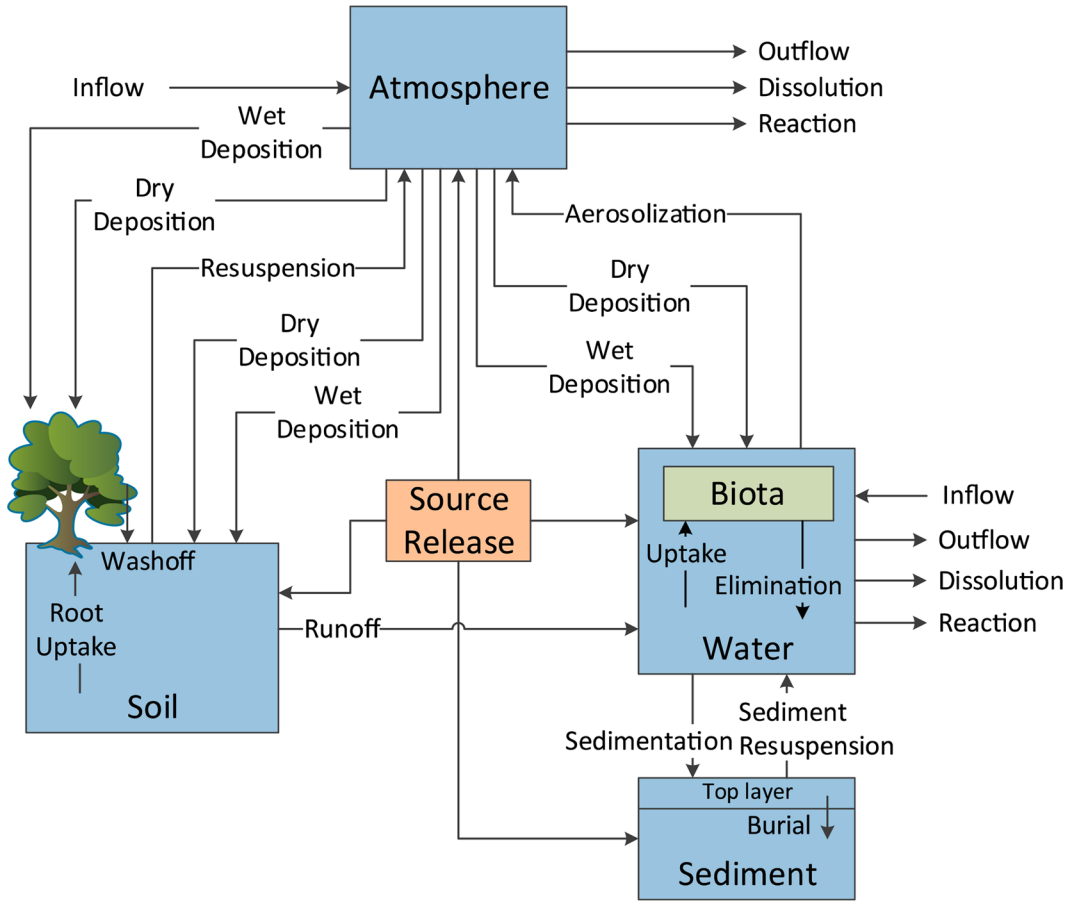

Figure 1. Environmental compartments and intermedia transport processes in a model multimedia environment.

expense of significant data needs regarding spatial distribution of various parameter (e.g., source emissions rates, local geography, and meteorology).[29,36]

The transport behavior of ENMs in the environment is governed by physical transport mechanisms of particulate matter. This is in contrast to chemical pollutants in gaseous and dissolved phases, whose interphase mass transport rates are governed by chemical potential (fugacity) driving forces that are constrained by thermodynamic equilibrium.[32] In contrast, the rates of ENMs' intermedia transport processes (e.g., dry deposition, rain scavenging, sedimentation) are governed by their particle size distribution (PSD).[37] Although multimedia models that incorporate mechanistic description of intermedia transport are yet unavailable, models have been proposed to describe the transport of ENMs in the soil[38] and aquatic environment (water and sediment).[22,39] For example, steady-state concentrations of TiO_2 in the Rhine River were estimated based on a model utilizing multiple water and sediment subcompartments.[22] While the above studies provided useful information, there is also a need for models to assess the potential distribution of ENMs in the multimedia environment and associated exposure concentrations for various ENMs release scenarios that may be of interest.

Accordingly, in order to assess environmental ENM exposure levels, a generalized compartmental multimedia fate and transport modeling framework was developed with the capability for expansion as the knowledgebase regarding ENMs further develops. Following the above approach, a model for the multimedia environmental distribution of nanomaterials (MendNano) is presented that enables estimations of the dynamic mass distributions and exposure concentrations of ENMs within and transport fluxes between various environmental media for a broad range of environmental scenarios of interest. A number of illustrative test cases are then discussed to elucidate the potential regional scale multimedia mass distribution, media concentrations, and significance of different transport pathways for selected ENMs.

MATERIALS AND METHODS

Modeling Approach. A multimedia compartmental modeling framework was developed for simulating the environmental distribution of ENMs. The present approach considers the environment as a collection of well-mixed compartments[32] each representing a specific medium (e.g., atmosphere, water, and top layer of soil and sediment) or biological entity (i.e., waterborne biota, vegetation), with intermedia mass transport between adjacent compartments (Figure 1). Multimedia compartmental models are suitable for a first tier assessment of potential environmental impact prior to engaging in more detailed and resource intensive use of spatial models or field monitoring.[29]

Model Equations. In order to describe the environmental multimedia distribution of ENM, the particle size distribution is discretized into a number of size fractions. The dynamic mass balance for each particle size fraction, k, for a given compartment is then written in the following general form

dx.doi.org/10.1021/es405132z | Environ. Sci. Technol. XXXX, XXX, XXX−XXX

$$\frac{d}{dt}[V_i C_{i,k}] = (Q_i^{in} C_{i,k}^{in} - Q_i^{out} C_{i,k}) + \sum_{\substack{j=1 \\ j\neq i}}^{M} \sum_{l=1}^{P} I_{i,j,k}^{l} + \sum_{n=1}^{U} R_{i,k}^{n} + S_{i,k} \quad k = 1...N;\ i = 1...T \tag{1}$$

where N is the number of particle size fractions, V_i [m^3] is the volume of compartment (or subcompartment) i, and $C_{i,k}$ [g m^{-3}] is the compartmental ENM concentration associated with particles in size fraction k. The first bracketed term on the right-hand side (RHS) of eq 1 represents advective mass transport, whereby Q_i^{in} and Q_i^{out} are advective flow rates [m^3 s^{-1}] in and out of compartment i (note: advection is applicable only for the air and water compartments), and $C_{i,k}^{in}$ is the inflow ENM concentrations [g m^{-3}]. Intermedia transport rates between compartments i and j, via transport process l, are represented by $I_{i,j,k}^{l}$ [g s^{-1}] with the net intermedia transport exchange rate (the second term on the RHS of eq 1) being the summed contributions of all processes (P) from all compartments (M) in contact (i.e., sharing a boundary) with compartment i. ENMs in the environment are subject to various transformation processes, such as dissolution, chemical reactions, and biological transformations,[40] whereby the rate of a given ENM transformation [g s^{-1}] n, in size fraction k in compartment i, is designated by $R_{i,k}^{n} = r_{i,k}^{n} V_i$, where $r_{i,k}^{n}$ is the volume specific ENM transformation rate [g m^{-3}]. For example, it has been reported that oxysulfidation of Ag,[41] oxidation of Fe,[42] and photodegradation of C_{60}[43] ENMs appear to follow first-order reaction kinetics. Also, at the expected low environmental concentrations of ENM,[26] a simple first-order process may often suffice for first tier analysis, whereby the transformation rate can be expressed as $R_{i,k}^{r} = \zeta_i K_{i,k}^{r} C_{i,k} V_i$, where $K_{i,k}^{r}$ [s^{-1}] is the transformation rate constant, and ζ_i is set as −1 or +1 for a consumption or production transformation, respectively. The rate constant for ENM transformation can be a function of a range of variables including, but not limited to, temperature, solution chemistry (e.g., pH, ionic species concentration, or the presence of natural organic matter (NOM)), ENM chemistry, and size. For physical transformation such as in the case of dissolution in the water compartment (i.e., $i = w$), for example, the rate of dissolution is given as $R_{w,k}^{diss} = K_{w,k}^{diss}(C_w^{(s)} - C_w^{(diss)})$, where $K_{w,k}^{diss}$ [m s^{-1}] is the ENM-environmental medium (e.g., water) mass transfer coefficient, which is a function of ENM size/geometry and chemistry, solution chemistry/composition, and flow hydrodynamics (Supporting Information (SI), *Dissolution*); $C_w^{(s)}$ is the ENM solubility [kg m^{-3}] that can be affected by factors such as media pH, temperature, ENM surface chemistry, and the ambient concentration of various species; $C_w^{(diss)}$ [kg m^{-3}] is the background mass concentration of the ENM dissolved in water; and $A_{T,k}$ [m^2] is the surface area of particle size fraction k (SI, *Dissolution*). The mass transfer coefficient can be predicted based on classical dissolution models which in the present simulations focused on dissolving spherical particles.[44] If experimental dissolution data (i.e., dissolution kinetics) are available, then these can be used to extract the needed mass transfer coefficient. Finally, $S_{i,k}$ is the ENM source release rate [g s^{-1}] of particles of size fraction k, to compartment i, and may be either time-invariant (i.e., constant) or temporally variable (SI, Figure S2).

Ambient particles are present (in both air and water) at significantly higher number concentrations relative to those which may be expected based solely on potential releases of ENMs.[22] Therefore, ENMs are likely to be associated with ambient particulates (due to various surface−surface interactions[37]) given the high available surface area of ambient particles and tendency of most ENMs to agglomerate.[39,45,46] Thus, intermedia transport associated with both air and water will be impacted by the ambient PSDs in the above media. It is well-known that ambient PSDs in air[47−49] and water[50,51] are self-preserving (i.e., similar over time). The particle size of ambient aerosols typically ranges from 0.001 to 2 μm with PSDs typically described by a trimodal log-normal size distribution.[49] Suspended solids in natural water bodies are typically in the size range of 0.01−1 μm for lakes,[52] 1−100 μm for oceans,[53] and 30−150 μm for rivers,[54] and log-normal size distributions have been often reported,[22] with a concentration range that can vary significantly (30 μg L^{-1}−200 mg L^{-1})[55,56] depending on the specific water body. The attachment efficiency of ENMs to ambient particles is thus an important factor that is likely to dictate the distribution of ENMs throughout the particulate phase in various environmental media. The attachment efficiency (i.e., typically defined as fraction of collisions that result in attachment/agglomeration[22,37]) is a complex parameter based on established theory of particle−particle interactions (e.g., the classical[57] and extended[58] DLVO theories, which describe particle−particle interactions due to attractive and repulsive interaction energies). However, fundamental predictions of ENM agglomeration (homogeneous and/or heterogeneous with ambient particles) based on the attachment efficiency (as predicted by DLVO/Extended DLVO) require solution of the Smoluchowski coagulation equation,[22,37] in which a single simulation instance may take many hours to days of CPU time.[37] Such complex models are less practical for screening level multimedia assessment (where a single simulation instance takes only minutes to complete). It is noted that the Smoluchowski equation was used in recent work on environmental ENMs transport with assumed values for the attachment efficiency.[22] Although the above did not provide *a priori* prediction of the agglomeration state based on predicted attachment efficiencies, reported simulation results suggest that, even with low attachment efficiency (0.01), essentially all ENMs would be attached to ambient particles.[22] In order to reduce the level of multimedia model complexity, yet retain a capability for exploring various levels of ENMs attachment to ambient particles, an "attachment factor" is introduced in the present work that is defined as the fraction of ENMs attached to ambient particles. ENMs are therefore allowed to distribute throughout the ambient particulate phase based on a specified attachment factor (SI, *ENM Attachment Factor*) that varies in the range of [0, 1] (i.e., no-attachment of ENMs to ambient particles to complete attachment) and may depend on water chemistry and ENM chemistry (for a given ENM and media conditions) as well as ENM and ambient particulate sizes.

Transport rates of ENMs between compartments, $I_{i,j,k}^{l}$ (eq 1), as depicted in Figure 1 can be described by various mechanistic intermedia transport process models as described in detail in the Supporting Information (SI, *Intermedia Transport Processes*). Briefly, dry deposition rate was determined based on the air phase PSD and dry deposition velocity to water,[59,60] soil,[60,61] and vegetative canopy.[60,62] The rate of precipitation scavenging (wet deposition) removal of particles from air[63] and required scavenging ratio were determined as a function of rainfall intensity and drop size distribution, while also accounting for

dx.doi.org/10.1021/es405132z | Environ. Sci. Technol. XXXX, XXX, XXX−XXX

the size distribution of airborne particles.[64] ENMs wash-off from foliage was determined based on water retention capacity of the vegetative foliage.[29] Wind resuspension rate was estimated by the Wind Erosion Equation (WEQ)[65] which accounts for soil properties; and soil loss due to runoff was estimated from the Revised Universal Soil Loss Equation based on soil erodibility and topographic factors.[66] Aerosolization (i.e., introduction of particles from water to air) was estimated with considerations of the effect of wind speed.[67] Sedimentation of particles suspended in water was determined by Stokes' settling while accounting for ENM agglomerates porosity,[37] and resuspension of sedimented particles can be estimated from models that consider current stress at the sediment surface induced by waves[68,69] or streamflow.[70] The rate of ENMs dissolution was estimated based on the classical diffusion model which in the present analysis focused on spherical particles[44] while considering the size distribution and porosity of the suspended agglomerates (SI, Table S8). Finally, the capability of exploring ENMs uptake by biota and plant roots is provided via a simple uptake rate model (SI, *Intermedia Transport Processes*), requiring uptake and elimination rate constants (e.g., as may be determined from available experimental ENMs uptake data).

The compartmental mass balance as given by eq 1 can be expressed in terms of the specific intermedia transport processes for the air (eq 2) and water (eq 3) compartments as

$$\frac{d}{dt}[V_a C_{a,k}] = I_{s,a}^{resusp} + I_{w,a,k}^{aerosol} - \sum_j I_{a,j,k}^{dry} - \sum_j I_{a,j,k}^{wet} + (Q_a^{in} C_{a,k}^{in} - Q_a^{out} C_{a,k}) + R_{a,k} + S_{a,k} \quad k = 1...N \tag{2}$$

$$\frac{d}{dt}[V_w C_{w,p}] = \sum_k I_{a,w,k}^{dry} + \sum_k I_{a,w,k}^{wet} + I_{sed,w}^{sedresusp} + I_{s,w}^{runoff} + I_b^{elim} - I_{w,sed}^{sed.} - I_{w,a,p}^{aerosol} - I_{w,b,p}^{uptake} + (Q_w^{in} C_{w,p}^{in} - Q_w^{out} C_{w,p}) + R_{w,p} - K_{i,k}^{diss}(C_w^{(s)} - C_w^{(diss)})A_{T,k} + S_{w,p} \quad p = 1...N \tag{3}$$

where the first four terms on the right-hand side (RHS) of eq 2 represent (in order) the ENMs rates of wind soil resuspension, aerosolization (from water), and atmospheric dry and wet (rain scavenging) deposition. The first eight terms on the RHS of eq 3 represent (in order) ENMs rates of atmospheric dry and wet deposition to water, sediment resuspension, runoff (from soil to water), elimination from biota, sedimentation, aerosolization, and uptake by biota. In the above equations subscripts *a, b, s, w,* and *sed,* refer (in order) to air, biota, soil, water, and sediment, and the indices *k* and *p* represent particle size fraction in air and water, respectively.

Retardation of ENMs infiltration in the soil matrix is enhanced when ENMs agglomerate, as expected under typical environmental conditions.[38] Consequently, ENMs are expected to accumulate primarily in the soil (and sediment) surface layer.[29] Studies have suggested that ENMs may penetrate only short distances into the soil column,[38,71] although detailed soil transport would clearly depend on specific soil conditions. Notwithstanding, for the purpose of estimating exposure concentrations, one may elect to calculate such concentrations based on a reasonable soil or sediment depth[72] over which the ENM mass is then assumed to distribute (e.g., SI, Tables S7, S8, S12). Consistent with the above argument, ENM mass at the soil, m_s, and sediment, m_{sed}, surface layers are tracked via the following mass balances

$$\frac{d}{dt}m_s = \sum_k I_{a,s,k}^{dry} + \sum_k I_{a,s,k}^{wet} + I_{f,s}^{washoff} - I_{s,a}^{resusp} - I_{s,w}^{runoff} - I_s^{root} + R_s + S_s \tag{4}$$

$$\frac{d}{dt}m_{sed} = I_{w,sed}^{sed.} - I_{sed,w}^{sedresusp} - I_{sed}^{burial} + R_{sed} + S_{sed} \tag{5}$$

where the first six terms on the RHS of eq 4 represent (in order) ENMs input rates to soil by dry and wet deposition, washoff from foliage (designated by subscript *f*), and removal by wind resuspension, runoff, and root uptake; the seventh and eighth terms represent ENMs transformation and source release rates, respectively. The five terms on the RHS of eq 5 represent, in order, the rates of ENMs sedimentation, resuspension from sediment, sediment burial, transformation, and source release.

Within the multimedia compartmental modeling framework, ecological receptors (e.g., plant, biota) can be represented as additional compartments.[28,29,32] In such a formulation, rates of accumulation of ENMs mass on vegetative foliage, m_f, and in root, m_{root}, can be represented by[29]

$$\frac{d}{dt}m_f = \sum_k I_{a,f,k}^{dry} + \sum_k I_{a,f,k}^{wet} - I_{f,s}^{washoff} \tag{6}$$

$$\frac{d}{dt}m_{root} = I_s^{root} \tag{7}$$

in which the terms on the RHS of eq 6 represent (in order) the rates of ENMs dry and wet deposition and washoff, and the term on the RHS of eq 7 represents ENMs removal from soil via root uptake. Efforts are currently underway to develop data and models of ENMs uptake via the root pathway,[73,74] and uptake rate constants need to be extracted from experimental data. In principle, one can also describe the accumulation of ENM mass, m_b, in biota via a compartmental mass balance

$$\frac{d}{dt}m_b = \sum_k I_{b,w,k}^{uptake} - I_b^{elim} \tag{8}$$

where the first and second terms on the RHS represent the rates of ENMs uptake and elimination by biota. Mechanistic models and/or experimental data for ENM accumulation in biota are in the developing stage, but nonetheless approximate treatment of uptake rate may be appropriate for a first tier analysis (SI, *Intermedia Transport Processes*). Alternatively, in the absence of uptake kinetics data, one may estimate the range of magnitude of concentrations in biota, using reported bioconcentration factors (BCFs; SI, Table S14), in conjunction with model predictions of ENM concentrations in water.

Simulations of the multimedia distribution of ENMs require specification of ENM properties, environmental compartment properties, meteorological parameters (e.g., monthly average temperature, wind speed, relative humidity, and rainfall data; SI, *Rain Event Generator*), intermedia transport process parameters, and source emission scenarios which can be set as temporally variable (SI, Figure S2). The modeled region is described by its dimensions and other geographical parameters. The volume of atmosphere compartment is set as $(A_{as} + A_{aw})H_{mix}$, where H_{mix} [m] is the atmospheric mixing height.[75] The mixing height can vary seasonally and diurnally, but an average monthly or annual

dx.doi.org/10.1021/es405132z | *Environ. Sci. Technol.* XXXX, XXX, XXX−XXX

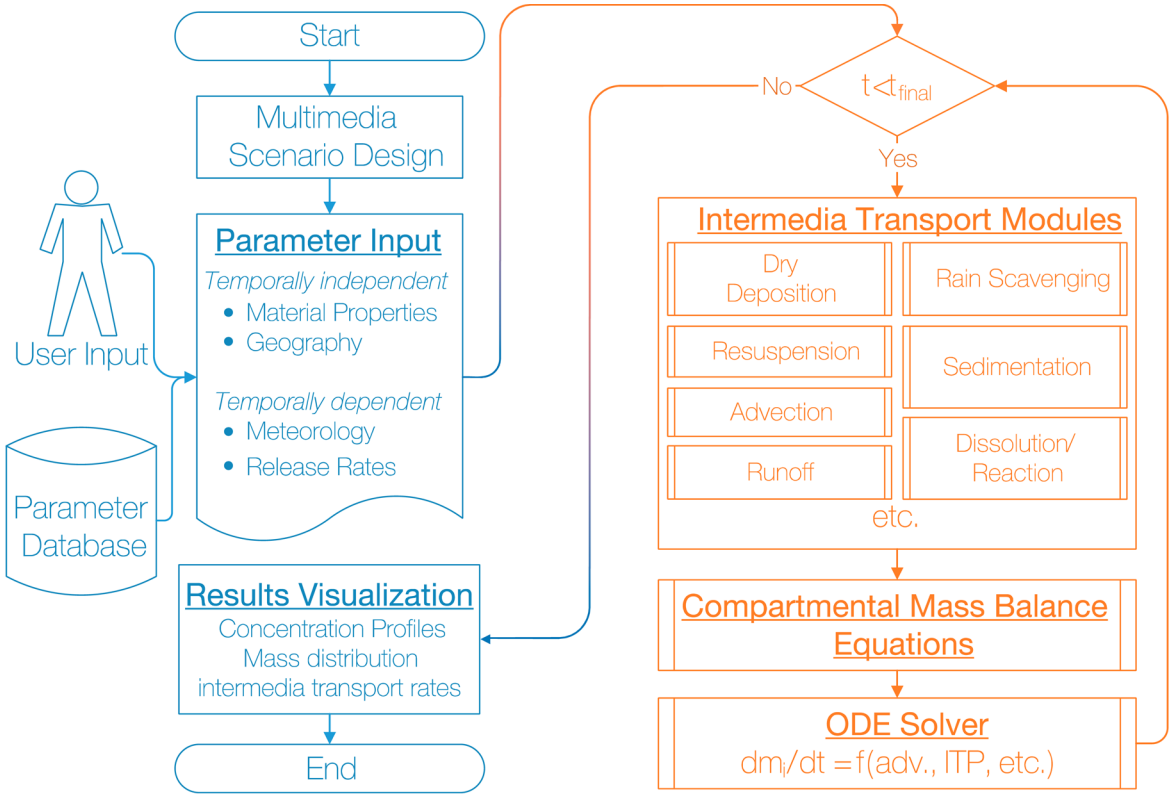

Figure 2. Overview of the MendNano modeling platform.

mixing height is often suitable for first tier analysis.[32] Note that it is reasonable to set $Q_i^{in} = Q_i^{out}$ and thus advective volumetric flow rates Q_i^c into the atmospheric and water compartments are expressed as $Q_i^c = V_i/\tau_{i_{res}}$, where V_i is the compartmental volume and $\tau_{i_{res}}$ [s] is the advective residence time. In the absence of information regarding $\tau_{i_{res}}$, one can set $Q_i^c = v_i^c \cdot A_i^c$, where v_i^c is the wind or current speed, and A_i^c is the cross-sectional compartmental area perpendicular to the prevailing wind or current direction. Surface area of the foliage compartment is expressed as $A_{as} \cdot \phi_{veg} \cdot F_f$ where ϕ_{veg} is the fraction of soil area, A_{as}, covered by vegetation (SI, Table S8), and F_f [m^2_{foliar} m^{-2}_{soil}] is the foliage area per unit area of soil.[76,77]

Model Structure. The MendNano modeling platform consists of the following modules: a) scenarios design and model parameter input, b) intermedia transport processes, c) model equations solver, and d) results visualization and reporting (Figure 2). The model was implemented as a Web-based application (using HTML, JavaScript, PHP, and MySQL) enabling execution of the numerical model (developed using MATLAB) on a remote server. [The Web implementation for MendNano is available at http://mendnano.polysep.ucla.edu/. Model codes and input data for all simulations discussed in the manuscript are available upon request and subject to appropriate material transfer agreements.] Required model input includes ENM and ambient particle properties, geographical parameters, meteorological parameters, and source release rates. Once a multimedia scenario is established the set of model ordinary differential mass balance equations (eqs 1−8) are solved along with the various intermedia transport submodels (SI, *Intermedia Transport Processes* and Table S1). Model simulations were carried out on a Linux based server (Intel Xeon 8-Core processors at 2.66 GHz, 64GB RAM), with a typical ∼3 min CPU time for a 1-year simulation.

Assessment of Modeling Approach Based on Simulations of the Multimedia Distribution of Particulate Matter. In order to assess the suitability of the present modeling approach for describing the dynamic multimedia distribution of particulate matter, simulations were first carried out for low volatility[78,79] and essentially water insoluble (solubility 0.26−2.7 $\mu g\ L^{-1}$)[80] polycyclic aromatic hydrocarbons (PAHs) (e.g., benzo[a]pyrene (B[a]P), benzo[ghi]-perylene (B[ghi]P), dibenz[a,h]anthracene (DBA)), which strongly adsorb onto particulate matter.[81,82] MendNano simulations for B[a]P, B[ghi]P, and DBA for the Southeast Ohio (US), Los Angeles (CA, US), and Birmingham (UK) regions, for which monitoring data were provided (SI, Figure S3), demonstrated agreement with field data, to within a factor of 2 or better, at the acceptable level for compartmental models (SI, *Assessment of Multimedia Compartmental Modeling Approach*).[83−85]

Test Cases of Multimedia Distributions of ENMs. MendNano simulations to illustrate the multimedia distribution of ENMs were carried out for selected ENMs including metal oxide (Al_2O_3, CeO_2, CuO, Fe_3O_4, TiO_2, ZnO), silver (Ag), nanoclays, silica (SiO_2), and carbon nanotubes (CNT) ENMs. The analyses included both multimedia distributions of the above ENMs on a country scale for U.S. and Switzerland as well as for a regional scale of the characteristics of Los Angeles County. ENM, regional, and meteorological parameters used in the simulations[86,87] are reported in the Supporting Information (SI, Tables S7−S13). All simulations were carried out for a period of at least one year.

Emission release rates for the ENMs of the present test cases were reported in the literature[26,27] based on life cycle inventory

dx.doi.org/10.1021/es405132z | Environ. Sci. Technol. XXXX, XXX, XXX−XXX

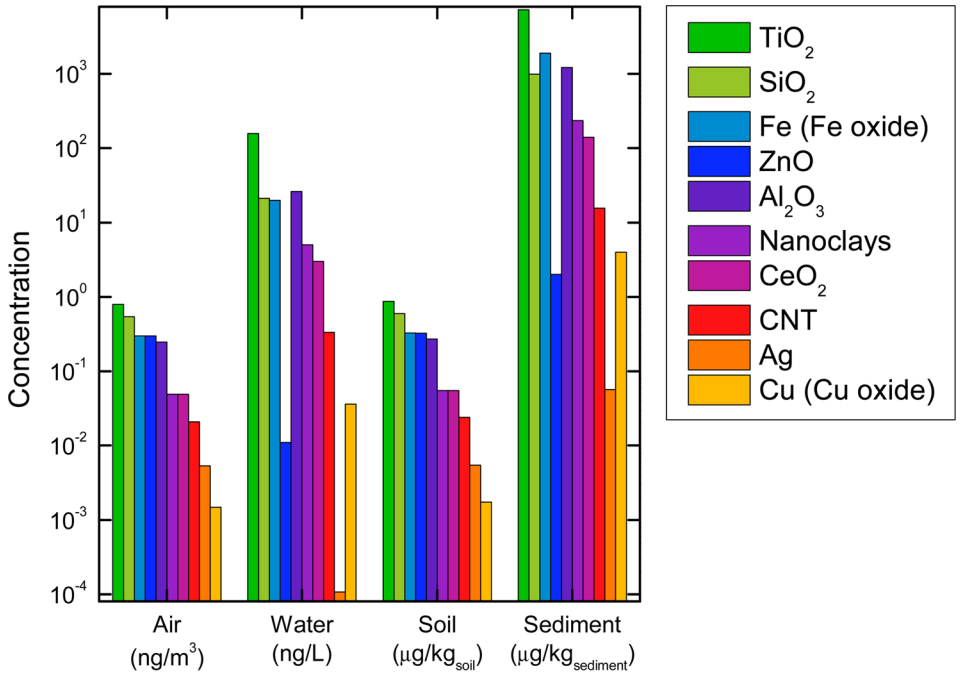

Figure 3. Predicted compartmental concentrations of Ag, Al_2O_3, CeO_2, CNT, Cu-based ENMs (metal and metal oxides), Fe-based ENMs (metal and metal oxides), nanoclays, SiO_2, TiO_2, and ZnO in the Los Angeles region at the end of 1-year simulation. ENM releases are to air and water only, and the release rates (to air and water) were estimated following the proposed regional scaling from published[24] estimates of global media-specific ENMs release rates (SI, Table S12) to the Los Angeles region and assuming no regional distribution of ENM releases to soil. (Note: Fe (Fe oxide), ZnO, Ag, and Cu (Cu oxide) solubilities are 0.001, 4.45, 1.9, and 0.002 mg L^{-1}, respectively; SI, Table S10).

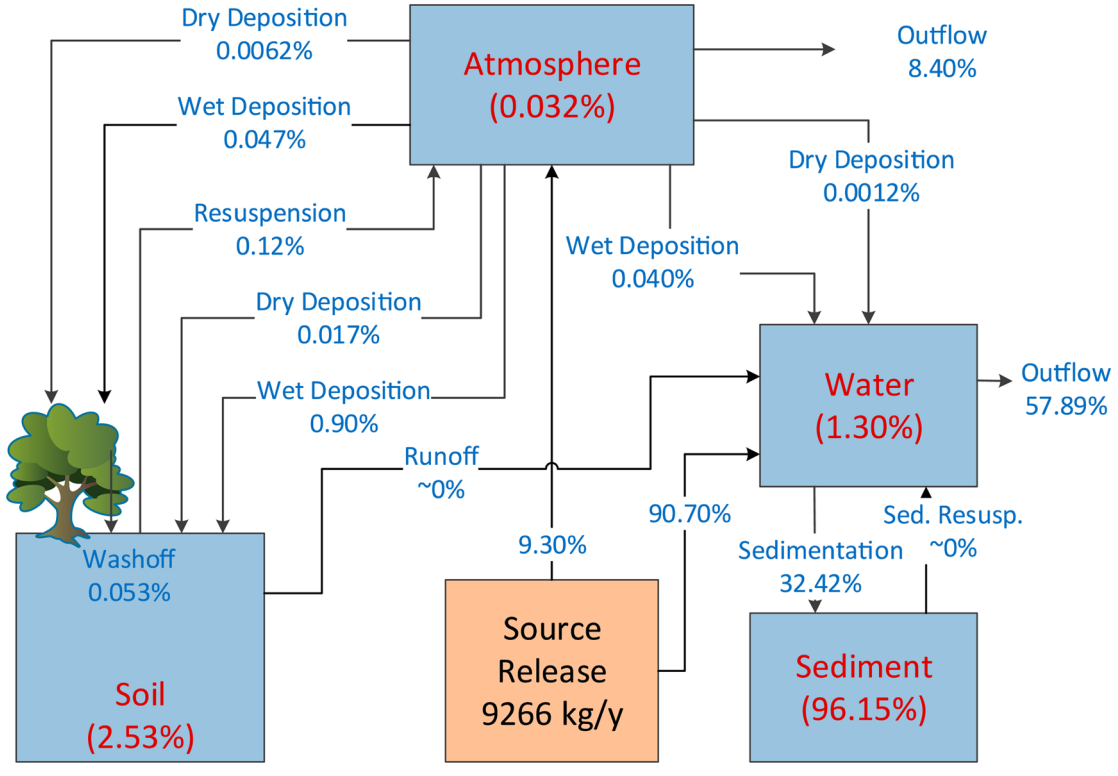

Figure 4. Intermedia transport rates of TiO_2 and mass distribution among the various compartments at the end of 1-year simulation for the Los Angeles test case. Simulation conditions (including release rates of TiO_2) are the same as in Figure 3. ENM intermedia transport rates are reported as percent (in blue font) of the total ENM source release rate (note: runoff and sediment resuspension are of the order of 10^{-6} % and 10^{-5} %, respectively). The percent of the total ENM mass in the multimedia system is also reported for each compartment (in red font within the parentheses).

dx.doi.org/10.1021/es405132z | Environ. Sci. Technol. XXXX, XXX, XXX−XXX

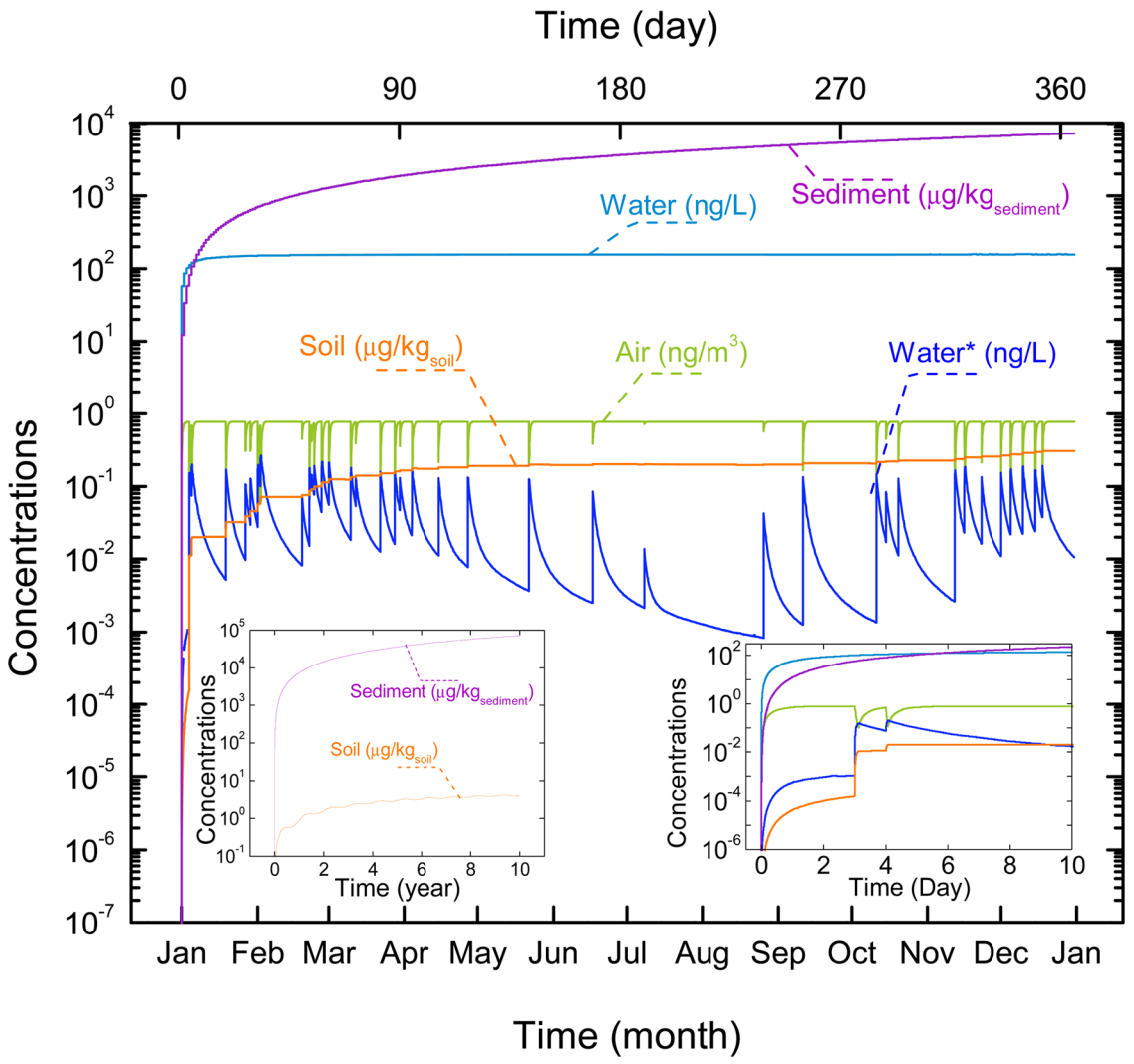

Figure 5. Temporal concentration profiles of TiO_2 in Los Angeles. Simulation conditions (including release rates of TiO_2) are the same as in Figure 3. Also reported is TiO_2 concentration profile in water for a scenario without direct release to water, denoted by the asterisk (*) and the corresponding curve. Inset figures: (left) concentration profiles for soil and sediment for 10 years and (right) concentration profiles for the first 10 days (day 0 to day 10).

assessment (LCIA) study[24] for the global release rates of Ag, Al_2O_3, CeO_2, CNT, Cu-based ENMs, Fe-based ENMs, nanoclay, SiO_2, TiO_2, and ZnO (SI, Table S13), which were reported based on estimated global production rates and expressed as percentages of the total production rates of the ENMs,[24] consistent with those reported elsewhere.[26] A recent study[88] suggested that regional release rates of ENMs can be estimated by scaling global ENM release rates on the basis of population and economic indicators if such are available. Accordingly, the above approach was utilized, in illustrative test case simulations for the Los Angeles region (SI, Table S8), to estimate media-specific ENM releases (SI, Table S13). Estimates of ENM release rates depend on various assumptions regarding production rates, ENM manufacturing, and use and disposal; thus, it is not surprising that a significant range of release estimates have been reported.[88−90] Nonetheless, LCIA estimates of ENM release rates are useful for first tier analysis of the multimedia distribution of ENMs. In this regard, it is noted that ENMs release to soil is often reported as the sum of two contributions: (1) releases from wastewater treatment plants (WWTP) and (2) "direct releases" (mostly during the "use" stage of the ENM life cycle).[24] ENMs release to soil by "direct release" was reported to account for about 8%[26] to 71%[24] of the total release to soil. However, it is unclear from published LCIA studies if "direct release" to soil is localized or represents ENM release that is regionally distributed. Additionally, it has been reported that in certain countries residuals from WWTP are not released to soil,[26] while in the US biosolids (i.e., WWTP sludge) are applied to less than 1% of the country's agricultural land.[91] Clearly, there is uncertainty as to the apportionment of local versus regional (if any) ENMs release to soil. At the same time, one should recognize the possibility of hot-spots that can result in elevated ENM concentrations in soil. While some MFA studies have assumed scenarios in which total ENMs releases to soil (including those from WWTP) are distributed over the entire soil in the region,[23,25−27] the validity of such an assumed scenario is questionable. Nonetheless, in the present study, the impacts of the above soil release scenarios with and without ENM release from WWTP (SI, Figures S4) and with and without "direct release" to soil (SI, Figures S6, S7, Table S17) were explored via MendNano simulations.

dx.doi.org/10.1021/es405132z | Environ. Sci. Technol. XXXX, XXX, XXX−XXX

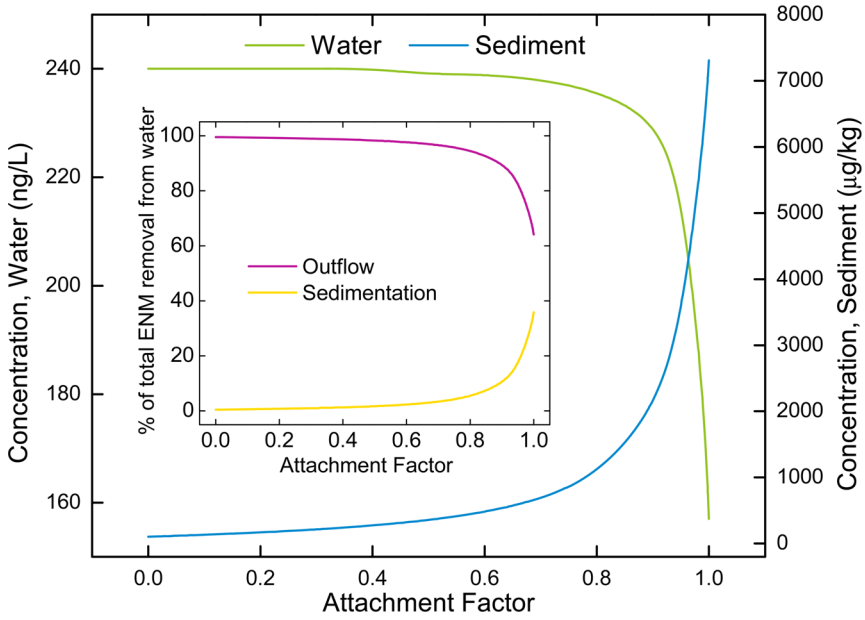

Figure 6. Impact of TiO_2 ENM attachment to suspended solids (in water) on ENM concentrations in water and sediment at the end of 1-year simulation. Inset: Percent ENM removal from water compartment due to advection and sedimentation. Geographical and meteorological conditions and release rates of TiO_2 are the same as in Figure 3. The initial log-normal PSD parameters for suspended ENMs: μ_{ln} = 5.7 nm, σ_{ln} = 0.4 nm.

RESULTS AND DISCUSSION

Significance of Intermedia Transport Pathways and Source Apportionment on Multimedia Distribution of ENMs. An illustration of the impact of regional meteorology and relative release rates of ENMs on their environmental distribution is provided in Figure 3 (also SI, Figure S6), based on simulations for selected metal and metal oxide, CNTs, and nanoclay ENMs, focusing on the Los Angeles region as an illustrative case. As expected, ranking of ENM concentrations in air follows (as expected) the order of increasing concentrations correlating with increased source release rates (SI, Table S13). Similarly, ranking of ENMs concentrations in water follows the order of release rates to water (SI, Table S13), with exception of the sparingly soluble ENMs (Fe (Fe oxide), ZnO, Ag, Cu (Cu Oxide)). The above behavior is attributed to the fact that ENMs release rate to water dominates any input from intermedia transport (i.e., atmospheric deposition and runoff) (Figure 4, SI, Figures S7, S8).

In the absence of direct ENMs release to soil, atmospheric deposition is the sole contributor to the mass of ENMs in soil, with percent ENM mass (relative to the total ENM mass in the environment) being in the range of 2.53−96.05% for the set of ENMs considered in the present study (SI, Table S17). The mass distribution of ENMs as shown in the example of Figure 4 for TiO_2 indicates only 2.53% of the total environmental mass of this ENM in soil with atmospheric wet deposition being the major ENM input to this compartment. When direct release to soil are considered, the percent mass of ENM in the soil can increase significantly (77.01−99.90%; SI, Table S17). Similarly, in the absence of direct ENM release to water, one would expect ranking of ENMs concentrations in water to also follow the ranking of release rates to air, given that ENMs input to water would also be primarily due to atmospheric deposition (Figure 4). With direct release to soil, compartmental concentrations (relative to the absence of direct ENM release to soil) would increase by factors of up to 3 and 106 in air and soil, respectively, and by up to 6% and 0.2% in water and sediment, respectively. At the same time, higher ENMs soil concentrations would result in correspondingly higher ENMs input rate to air by wind resuspension as depicted for the example of TiO_2 distribution (SI, Figure S7) and also evident in the mass distribution of the various evaluated ENMs (SI, Table S17). It is also noted, as shown in the Los Angeles example, simulations for TiO_2 (SI, Figure S10) as the fraction of total ENM release to soil, which is apportioned for regional distribution (i.e., over the soil), is increased from zero (i.e., equivalent to the case of confined local release) to 100% (i.e., complete regional distribution); TiO_2 concentrations in air and soil increase by factors of 5.8 and 236, respectively. Clearly, the multimedia mass distribution of ENMs can be significantly impacted by the apportionment of the total estimated release rates among the different media. For example, simulation of TiO_2 distribution for the Los Angeles test case (SI, Figure S9) indicates percent of total regional ENM mass in water and sediment that decreased significantly from 0.66% to 0.01% and from 49.25% to 2.06%, respectively, as the ratio of ENM release to air relative to water decreased from 4:1 to 1:0 (i.e., 100% release to air).

The dynamic evolution of the compartmental concentrations (and thus mass distribution) is illustrated in the example of Figure 5 for an ENM with a size distribution patterned after TiO_2 but with release rate only to air and water. It is apparent that ENM concentrations in air and water approach steady state behavior over short periods of 72 h and 8 days, respectively. ENM concentrations in air fluctuate markedly with rain events during which there is rapid reduction in the atmospheric ENM concentrations, followed by a rise to steady-state value after each event. In contrast, ENM concentrations in soil increases continually with each rain event adding to the total ENMs mass accumulation in the soil. For example, for the simulation that starts on January 1st, the ENM concentration in soil rapidly rises within about 4 months and subsequently increases slowly over time with continuing input of ENMs to soil from wet scavenging as well as dry deposition (inset in Figure 5); in the

dx.doi.org/10.1021/es405132z | Environ. Sci. Technol. XXXX, XXX, XXX−XXX

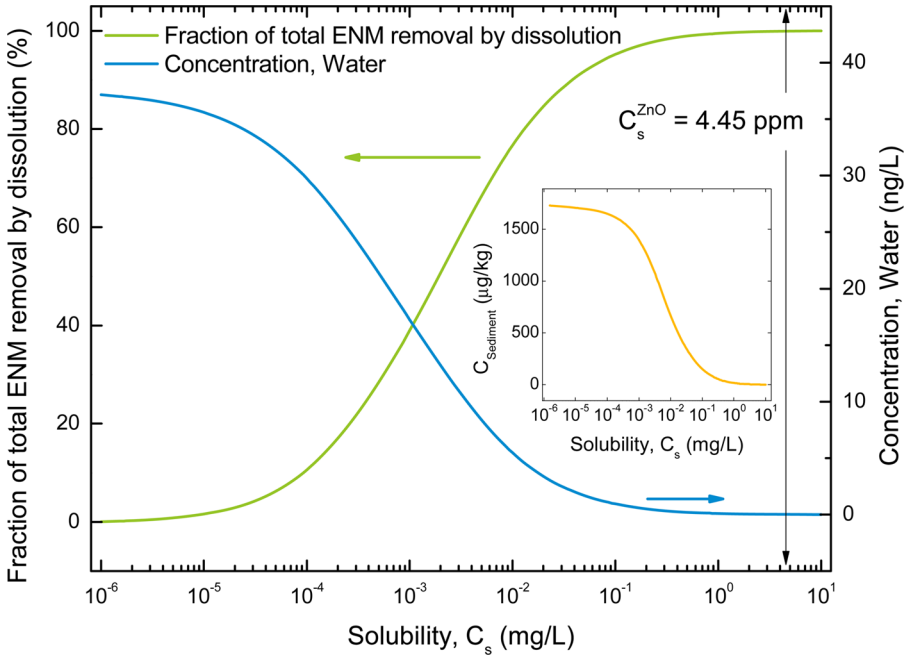

Figure 7. Contribution (%) of dissolution to total ENM removal and ENM concentrations in water and sediment (inset) as functions of solubility at the end of 1-year simulation. Simulation conditions (with release rates of ZnO, ambient PSD, and regional parameters) are the same as in Figure 3. The ionic diffusivity of 6.7×10^{-10} m^2 s^{-1} is used, which is a typical value for a range of metallic ions, including Zn^{2+}.[96]

above specific simulation steady state would not be expected to occur until after about 10 years. Input of ENMs to sediment also continues to increase over time (Figure 5). In the absence of direct release to water, one would expect episodic inputs from wet scavenging to lead to periodic increases in the ENM water concentration that would subside after rain events (primarily due to advection from the water compartment).

Effect of Nanomaterial Attachment to Ambient Particulates. Although there have been numerous studies on the attachment efficiency of ENMs,[45] data and predictive models of ENMs association with ambient particles (in air and in water) under environmental conditions are lacking.[22,39] Therefore, in the present modeling approach, ENM association with ambient particles was incorporated via an attachment factor (as defined per eq S26 (SI)). An illustration of the attachment factor impact on ENM concentration in water and sediment is provided in Figure 6 (also for the Los Angeles Region) for ENM of properties and emission rates patterned based on TiO_2 as in the simulation of Figure 5. It is apparent that once the attachment factor increases to above ~0.7, predicted ENM concentration in water decreases rapidly, while correspondingly ENM concentration in sediment increases. Over the attachment factor range of [0:1] predicted ENM concentrations increase in water and decrease in sediment by factors of 1.5 and 69, respectively. The above behavior is due to the greater effect of sedimentation on ENM removal from the water column with increased ENMs attachment to larger ambient suspended solids (SI, *Sedimentation*). ENMs removal from the water compartment via advection (i.e., currents, tidal flow) is influenced by partitioning of ENMs to suspended ambient particles. This behavior is illustrated in the inset in Figure 6, which demonstrates that as the attachment factor increases the percent of ENMs removal (relative to the total input) via advection decreases, given the lower concentration in water due to increased ENMs removal by sedimentation. Overall, however, advective ENM removal from water column is ~2−200 times greater than removal by sedimentation. ENMs association with ambient atmospheric aerosols can also impact the dynamic multimedia distribution of ENMs. For example, for the same conditions as in Figure 5, simulations over a range of values of the attachment factor for ENMs in the air phase (SI, Figure S11) from 0 (i.e., no attachment to ambient aerosols) to unity revealed decreased dry and wet deposition rates by 52% and 10%, respectively, with little effect on the atmospheric concentration given the dominance of advective transport as a mechanism for ENM removal from the modeled region (see Figure 4).

Effect of Nanomaterial Dissolution on Environmental Distribution of ENMs. Nanomaterials are generally regarded as being water insoluble; however, certain ENMs can exhibit significant aqueous solubility (e.g., ZnO, Ag, CuO, Fe_3O_4),[92−96] which can enhance their loss (transformation) as suspended ENMs in water leading to lower concentration of these suspended ENMs in the water and sediment (SI, Figure S12). An illustration of the impact of dissolution on ENM loss (from the water column) is shown in Figure 7 for the same conditions as for the ZnO example in Figure 3 and with the ENM solubility as a simulation variable. Dissolution has a low impact on the ENMs loss from the water column (≤5%) when the ENM solubility is below ~5×10^{-5} mg L^{-1}. The concentration of suspended ENMs in water decreases with increased ENM solubility, and for the present example, this concentration would decrease by ~3 orders of magnitude (from 37.3 ng L^{-1} to 0.011 ng L^{-1}) as one progresses away from the condition of essentially insoluble ENMs (i.e., solubility ≤10^{-6} mg L^{-1}) to sparingly soluble ENMs such as ZnO (aqueous solubility ~4.45 mg L^{-1} at ~pH 8).[92] For the case of ZnO, the driving force for dissolution is sufficiently large (given that the background zinc ion concentration in natural water bodies is a few orders of magnitudes lower than ZnO solubility),[97] which is expected to result in essentially total dissolution of this ENM. In general, increased ENM dissolution will correspondingly reduce the

dx.doi.org/10.1021/es405132z | *Environ. Sci. Technol.* XXXX, XXX, XXX−XXX

accumulation of ENMs onto the sediment (Figure 7). When the ENMs are freely suspended in the water compartment (i.e., not attached to suspended ambient suspended solids) one should expect a higher ENM particle loss (due to increased dissolution) for the smaller ENM particles (given that particle area/volume ratio $\propto$ 1/diameter; also see SI, eq S16). However, accumulation of ENM particles on the sediment will be affected to a greater degree by a higher settling rate of larger freely suspended particles.

In summary, it is envisioned that environmental multimedia analysis can become an important tool in a tiered approach to environmental impact assessment and as a complement to life cycle assessment. Moreover, analysis of the multimedia distribution of ENMs that accounts for environmental intermedia transport processes can (a) assist in quantifying the contribution of the different intermedia transport pathways to the environmental distribution of ENMs, (b) enable estimation of ENM release given available field concentration data, and (c) allow for rapid "what-if" analyses.

■ ASSOCIATED CONTENT

Supporting Information

Simulation information including details regarding intermedia transport processes, source release rate scenarios, rain simulations, and media-specific ENMs release rates as well as ENM production estimations and additional results. This material is available free of charge via the Internet at http://pubs.acs.org.

■ AUTHOR INFORMATION

Corresponding Author

*Phone: 310-825-8766. Fax: 310-204-0095. E-mail: yoram@ucla.edu.

Notes

The authors declare no competing financial interest.

■ ACKNOWLEDGMENTS

This work was supported, in part, by the National Science Foundation and the Environmental Protection Agency under Cooperative Agreement Number DBI 0830117. Any opinions, findings, conclusions, or recommendations expressed herein are those of the author(s) and do not necessarily reflect the views of the National Science Foundation or the Environmental Protection Agency. This work has not been subjected to an EPA peer and policy review.

■ REFERENCES

(1) Cattaneo, A. G.; Gornati, R.; Sabbioni, E.; Chiriva-Internati, M.; Cobos, E.; Jenkins, M. R.; Bernardini, G. Nanotechnology and Human Health: Risks and Benefits. *J. Appl. Toxicol.* **2010**, *30*, 730−744.

(2) George, S.; Xia, T. A.; Rallo, R.; Zhao, Y.; Ji, Z. X.; Lin, S. J.; Wang, X.; Zhang, H. Y.; France, B.; Schoenfeld, D.; Damoiseaux, R.; Liu, R.; Lin, S.; Bradley, K. A.; Cohen, Y.; Nal, A. E. Use of a High-Throughput Screening Approach Coupled with In Vivo Zebrafish Embryo Screening To Develop Hazard Ranking for Engineered Nanomaterials. *ACS Nano* **2011**, *5*, 1805−1817.

(3) Jiang, W.; Kim, B. Y. S.; Rutka, J. T.; Chan, W. C. W. Nanoparticle-Mediated Cellular Response Is Size-Dependent. *Nat. Nanotechnol.* **2008**, *3*, 145−150.

(4) Kahru, A.; Dubourguier, H. C. From Ecotoxicology to Nanoecotoxicology. *Toxicology* **2010**, *269*, 105−119.

(5) Lin, S. J.; Zhao, Y.; Xia, T.; Meng, H.; Ji, Z. X.; Liu, R.; George, S.; Xiong, S. J.; Wang, X.; Zhang, H. Y.; Pokhrel, S.; Madler, L.; Damoiseaux, R.; Lin, S.; Nel, A. E. High Content Screening in Zebrafish Speeds up Hazard Ranking of Transition Metal Oxide Nanoparticles. *ACS Nano* **2011**, *5*, 7284−7295.

(6) Nel, A.; Xia, T.; Madler, L.; Li, N. Toxic Potential of Materials at the Nanolevel. *Science* **2006**, *311*, 622−627.

(7) Rallo, R.; France, B.; Liu, R.; Nair, S.; George, S.; Damoiseaux, R.; Giralt, F.; Nel, A.; Bradley, K.; Cohen, Y. Self-Organizing Map Analysis of Toxicity-Related Cell Signaling Pathways for Metal and Metal Oxide Nanoparticles. *Environ. Sci. Technol.* **2011**, *45*, 1695−1702.

(8) Ray, P. C.; Yu, H. T.; Fu, P. P. Toxicity and Environmental Risks of Nanomaterials: Challenges and Future Needs. *J. Environ. Sci. Health, Part C: Environ. Carcinog. Ecotoxicol. Rev.* **2009**, *27*, 1−35.

(9) Zhang, H. Y.; Ji, Z. X.; Xia, T.; Meng, H.; Low-Kam, C.; Liu, R.; Pokhrel, S.; Lin, S. J.; Wang, X.; Liao, Y. P.; Wang, M. Y.; Li, L. J.; Rallo, R.; Damoiseaux, R.; Telesca, D.; Madler, L.; Cohen, Y.; Zink, J. I.; Nel, A. E. Use of Metal Oxide Nanoparticle Band Gap To Develop a Predictive Paradigm for Oxidative Stress and Acute Pulmonary Inflammation. *ACS Nano* **2012**, *6*, 4349−4368.

(10) Zhang, H. Y.; Xia, T.; Meng, H.; Xue, M.; George, S.; Ji, Z. X.; Wang, X.; Liu, R.; Wang, M. Y.; France, B.; Rallo, R.; Damoiseaux, R.; Cohen, Y.; Bradley, K. A.; Zink, J. I.; Nel, A. E. Differential Expression of Syndecan-1 Mediates Cationic Nanoparticle Toxicity in Undifferentiated versus Differentiated Normal Human Bronchial Epithelial Cells. *ACS Nano* **2011**, *5*, 2756−2769.

(11) Cohen, Y.; Rallo, R.; Liu, R.; Liu, H. H. In Silico Analysis of Nanomaterials Hazard and Risk. *Acc. Chem. Res.* **2013**, *46*, 802−812.

(12) Colvin, V. L. The Potential Environmental Impact of Engineered Nanomaterials. *Nat. Biotechnol.* **2003**, *21*, 1166−1170.

(13) Gerber, C.; Lang, H. P. How the Doors to the Nanoworld Were Opened. *Nat. Nanotechnol.* **2006**, *1*, 3−5.

(14) Scown, T. M.; van Aerle, R.; Tyler, C. R. Review: Do Engineered Nanoparticles Pose a Significant Threat to the Aquatic Environment? *Crit. Rev. Toxicol.* **2010**, *40*, 653−670.

(15) Money, E. S.; Reckhow, K. H.; Wiesner, M. R. The Use of Bayesian Networks for Nanoparticle Risk Forecasting: Model Formulation and Baseline Evaluation. *Sci. Total Environ.* **2012**, *426*, 436−445.

(16) Hendren, C. O.; Badireddy, A. R.; Casman, E.; Wiesner, M. R. Modeling Nanomaterial Fate in Wastewater Treatment: Monte Carlo Simulation of Silver Nanoparticles (Nano-Ag). *Sci. Total Environ.* **2013**, *449*, 418−425.

(17) Hendren, C. O.; Lowry, M.; Grieger, K. D.; Money, E. S.; Johnston, J. M.; Wiesner, M. R.; Beaulieu, S. M. Modeling Approaches for Characterizing and Evaluating Environmental Exposure to Engineered Nanomaterials in Support of Risk-Based Decision Making. *Environ. Sci. Technol.* **2013**, *47*, 1190−1205.

(18) Boxall, A. B. A.; Chaudhry, Q.; Sinclair, C.; Jones, A.; Aitken, R.; Jefferson, B.; Watts, C. *Current and Future Predicted Environmental Exposure to Engineered Nanoparticles*; Central Science Laboratory: York, UK, 2007.

(19) von der Kammer, F.; Ferguson, P. L.; Holden, P. A.; Masion, A.; Rogers, K. R.; Klaine, S. J.; Koelmans, A. A.; Horne, N.; Unrine, J. M. Analysis of Engineered Nanomaterials in Complex Matrices (Environment and Biota): General Considerations and Conceptual Case Studies. *Environ. Toxicol. Chem.* **2012**, *31*, 32−49.

(20) Klaine, S. J.; Koelmans, A. A.; Horne, N.; Carley, S.; Handy, R. D.; Kapustka, L.; Nowack, B.; von der Kammer, F. Paradigms To Assess the Environmental Impact of Manufactured Nanomaterials. *Environ. Toxicol. Chem.* **2012**, *31*, 3−14.

(21) Weinberg, H.; Galyean, A.; Leopold, M. Evaluating Engineered Nanoparticles in Natural Waters. *TrAC, Trends Anal. Chem.* **2011**, *30*, 72−83.

(22) Praetorius, A.; Scheringer, M.; Hungerbuhler, K. Development of Environmental Fate Models for Engineered Nanoparticles-A Case Study of TiO2 Nanoparticles in the Rhine River. *Environ. Sci. Technol.* **2012**, *46*, 6705−6713.

(23) Mueller, N. C.; Nowack, B. Exposure Modeling of Engineered Nanoparticles in the Environment. *Environ. Sci. Technol.* **2008**, *42*, 4447−4453.

(24) Keller, A.; McFerran, S.; Lazareva, A.; Suh, S. Global Life Cycle Releases of Engineered Nanomaterials. *J. Nanopart. Res.* **2013**, *15*, 1−17.
(25) Gottschalk, F.; Scholz, R. W.; Nowack, B. Probabilistic Material Flow Modeling for Assessing the Environmental Exposure to Compounds: Methodology and an Application to Engineered Nano-TiO(2) Particles. *Environ. Modell. Software* **2010**, *25*, 320−332.
(26) Gottschalk, F.; Sonderer, T.; Scholz, R. W.; Nowack, B. Modeled Environmental Concentrations of Engineered Nanomaterials (TiO2, ZnO, Ag, CNT, Fullerenes) for Different Regions. *Environ. Sci. Technol.* **2009**, *43*, 9216−9222.
(27) Gottschalk, F.; Sonderer, T.; Scholz, R. W.; Nowack, B. Possibilities and Limitations of Modeling Environmental Exposure to Engineered Nanomaterials by Probabilistic Material Flow Analysis. *Environ. Toxicol. Chem.* **2010**, *29*, 1036−1048.
(28) Cohen, Y.; Cooter, E. J. Multimedia Environmental Distribution of Toxics (Mend-Tox). II: Software Implementation and Case Studies. *Pract. Period. Hazard., Toxic, Radioact. Waste Manage.* **2002**, *6*, 87−101.
(29) Cohen, Y.; Cooter, E. J. Multimedia Environmental Distribution of Toxics (Mend-Tox). I: Hybrid Compartmental-Spatial Modeling Framework. *Pract. Period. Hazard., Toxic, Radioact. Waste Manage.* **2002**, *6*, 70−86.
(30) Mackay, D.; MacLeod, M. Multimedia Environmental Models. *Pract. Period. Hazard., Toxic, Radioact. Waste Manage.* **2002**, *6*, 63−69.
(31) MacLeod, M.; Scheringer, M.; McKone, T. E.; Hungerbuhler, K. The State of Multimedia Mass-Balance Modeling in Environmental Science and Decision-Making. *Environ. Sci. Technol.* **2010**, *44*, 8360−8364.
(32) Mackay, D. *Multimedia environmental models: the fugacity approach*, 2nd ed.; Lewis Publishers: Boca Raton, FL, 2001; p 261.
(33) USEPA Testing for Field Applicability of Chemical Exposure Models. In *Workshop on Field Applicability Testing*; US Environmental Protection Agency: Athens, GA, USA, 1982.
(34) Kauffman, R.; Lee, M.; Murphy, R.; Burch, D.; Fisher, M.; Benjamin, A.; Jones, B. *Evaluation of TRIM.FaTE*; USEPA, Office of Air Quality Planning and Standards, Emissions Standards & Air Quality Strategies and Standards Divisions, Eds.; Research Triangle Park, NC, 2004; Vol. Vol. III - Model Comparison Focusing on Dioxin Test Case.
(35) Pistocchi, A. Some Considerations on the Use of Simple Box Models of Contaminant Fate in Soils. *Environ. Monit. Assess.* **2013**, *185*, 2855−2867.
(36) Mackay, D.; Paterson, S. Evaluating the Multimedia Fate of Organic-Chemicals - a Level-Iii Fugacity Model. *Environ. Sci. Technol.* **1991**, *25*, 427−436.
(37) Liu, H. H.; Surawanvijit, S.; Rallo, R.; Orkoulas, G.; Cohen, Y. Analysis of Nanoparticle Agglomeration in Aqueous Suspensions via Constant-Number Monte Carlo Simulation. *Environ. Sci. Technol.* **2011**, *45*, 9284−9292.
(38) Darlington, T. K.; Neigh, A. M.; Spencer, M. T.; Nguyen, O. T.; Oldenburg, S. J. Nanoparticle Characteristics Affecting Environmental Fate and Transport through Soil. *Environ. Toxicol. Chem.* **2009**, *28*, 1191−1199.
(39) Arvidsson, R.; Molander, S.; Sandén, B. A.; Hassellöv, M. Challenges in Exposure Modeling of Nanoparticles in Aquatic Environments. *Hum. Ecol. Risk Assess.* **2011**, *17*, 245−262.
(40) Lowry, G. V.; Gregory, K. B.; Apte, S. C.; Lead, J. R. Transformations of Nanomaterials in the Environment. *Environ. Sci. Technol.* **2012**, *46*, 6893−6899.
(41) Liu, J.; Pennell, K. G.; Hurt, R. H. Kinetics and Mechanisms of Nanosilver Oxysulfidation. *Environ. Sci. Technol.* **2011**, *45*, 7345−7353.
(42) Liu, Y.; Majetich, S. A.; Tilton, R. D.; Sholl, D. S.; Lowry, G. V. TCE Dechlorination Rates, Pathways, and Efficiency of Nanoscale Iron Particles with Different Properties. *Environ. Sci. Technol.* **2005**, *39*, 1338−1345.
(43) Hou, W.-C.; Jafvert, C. T. Photochemical Transformation of Aqueous C60 Clusters in Sunlight. *Environ. Sci. Technol.* **2008**, *43*, 362−367.
(44) Bird, R. B.; Stewart, W. E.; Lightfoot, E. N. *Transport phenomena*, 2nd ed., Wiley international ed.; J. Wiley: New York, 2007; p xii, 895p.
(45) Petosa, A. R.; Jaisi, D. P.; Quevedo, I. R.; Elimelech, M.; Tufenkji, N. Aggregation and Deposition of Engineered Nanomaterials in Aquatic Environments: Role of Physicochemical Interactions. *Environ. Sci. Technol.* **2010**, *44*, 6532−6549.
(46) Brant, J.; Lecoanet, H.; Wiesner, M. R. Aggregation and deposition characteristics of fullerene nanoparticles in aqueous systems. *J. Nanopart. Res.* **2005**, *7*, 545−553.
(47) Friedlander, S. K. *Smoke, dust, and haze: fundamentals of aerosol dynamics*, 2nd ed.; Oxford University Press: New York, 2000; p xx, 407p.
(48) Friedlander, S. K.; Wang, C. S. Self-Preserving Particle Size Distribution for Coagulation by Brownian Motion. *J. Colloid Interface Sci.* **1966**, *22*, 126−&.
(49) Seinfeld, J. H.; Pandis, S. N. *Atmospheric chemistry and physics: from air pollution to climate change*, 2nd ed.; J. Wiley: Hoboken, NJ, 2006; p xxviii, 1203 p.
(50) Farley, K. J.; Morel, F. M. M. Role of Coagulation in the Kinetics of Sedimentation. *Environ. Sci. Technol.* **1986**, *20*, 187−195.
(51) Spicer, P. T.; Pratsinis, S. E. Coagulation and Fragmentation: Universal Steady-State Particle-Size Distribution. *AIChE J.* **1996**, *42*, 1612−1620.
(52) Walther, C.; Büchner, S.; Filella, M.; Chanudet, V. Probing Particle Size Distributions in Natural Surface Waters from 15 nm to 2 μm by a Combination of LIBD and Single-Particle Counting. *J. Colloid Interface Sci.* **2006**, *301*, 532−537.
(53) Reynolds, R. A.; Stramski, D.; Wright, V. M.; Woźniak, S. B. Measurements and Characterization of Particle Size Distributions in Coastal Waters. *J. Geophys. Res.: Oceans* **2010**, *115*, C08024.
(54) Walling, D. E.; Moorehead, P. W. The Particle Size Characteristics of Fluvial Suspended Sediment: An Overview. *Hydrobiologia* **1989**, *176−177*, 125−149.
(55) Jacobs, M. B.; Ewing, M. Suspended Particulate Matter: Concentration in the Major Oceans. *Science* **1969**, *163*, 380−383.
(56) Susfalk, R. B.; Fitzgerald, B.; Knust, A. M. *Characterization of Turbidty and Total Suspended Solids in the Upper Carson River, Nevada*; Protection, N. D. o. E., Ed.; 2008.
(57) Hunter, R. J. *Foundations of colloid science*, 2nd ed.; Oxford University Press: Oxford; New York, 2001; p xii, 806p.
(58) Elimelech, M. *Particle deposition and aggregation: measurement, modelling, and simulation*; Butterworth-Heinemann: Oxford, England; Boston, 1995; p xv, 441p.
(59) Williams, R. M. A Model for the Dry Deposition of Particles to Natural-Water Surfaces. *Atmos. Environ.* **1982**, *16*, 1933−1938.
(60) Giorgi, F. A Particle Dry-Deposition Parameterization Scheme for Use in Tracer Transport Models. *J. Geophys. Res.: Atmos.* **1986**, *91*, 9794−9806.
(61) Sehmel, G. A.; Hodgson, W. H. *A model for predicting dry deposition of particles and gases to environmental surfaces*; 1978; p Medium: P; Size: 44pp.
(62) Slinn, W. G. N. Predictions for Particle Deposition to Vegetative Canopies. *Atmos. Environ.* **1982**, *16*, 1785−1794.
(63) Ryan, P. Review of Mathematical Models for Health Risk Assessment: IV. Intermedia Chemical Transport. *Environ. Software* **1993**, *8*, 157−172.
(64) Tsai, W.; Cohen, Y.; Sakugawa, H.; Kaplan, I. R. Dynamic Partitioning of Semivolatile Organics in Gas/Particle/Rain Phases during Rain Scavenging. *Environ. Sci. Technol.* **1991**, *25*, 2012−2023.
(65) USDA-ARS *A universal equation for measuring wind erosion*; United States Department of Agriculture - Agriculture Research Service, Ed.; 1961; pp 22−69.
(66) Renard, K. G.; Foster, G. R.; Weesies, G. A. *Predicting soil erosion by water: a guide to conservation planning with the Revised Universal Soil Loss Equation (RUSLE)*; USDA: WA, 1997.
(67) O'Dowd, C. D.; de Leeuw, G. Marine aerosol production: a review of the current knowledge. *Philos. Trans. R. Soc. A* **2007**, *365*, 1753−1774.

(68) Luettich, R. A.; Harleman, D. R. F.; Somlyody, L. Dynamic Behavior of Suspended Sediment Concentrations in a Shallow Lake Perturbed by Episodic Wind Events. *Limnol. Oceanogr.* **1990**, *35*, 1050−1067.
(69) Li, J.; Zhang, C. Sediment Resuspension and Implications for Turbidity Maximum in the Changjiang Estuary. *Mar. Geol.* **1998**, *148*, 117−124.
(70) Grant, W. D.; Madsen, O. S. Combined Wave and Current Interaction with a Rough Bottom. *J. Geophys. Res.: Oceans* **1979**, *84*, 1797−1808.
(71) Jaisi, D. P.; Elimelech, M. Single-Walled Carbon Nanotubes Exhibit Limited Transport in Soil Columns. *Environ. Sci. Technol.* **2009**, *43*, 9161−9166.
(72) ECB, *Technical Guidance Document on Risk Assessment*. European Chemicals Bureau, Institute for Health and Consumer Protection. European Commission: Dublin, 2003.
(73) Priester, J. H.; Ge, Y.; Mielke, R. E.; Horst, A. M.; Moritz, S. C.; Espinosa, K.; Gelb, J.; Walker, S. L.; Nisbet, R. M.; An, Y.-J.; Schimel, J. P.; Palmer, R. G.; Hernandez-Viezcas, J. A.; Zhao, L.; Gardea-Torresdey, J. L.; Holden, P. A. Soybean Susceptibility to Manufactured Nanomaterials with Evidence for Food Quality and Soil Fertility Interruption. *Proc. Natl. Acad. Sci.* **2012**, *109*, E2451−E2456.
(74) Rico, C. M.; Majumdar, S.; Duarte-Gardea, M.; Peralta-Videa, J. R.; Gardea-Torresdey, J. L. Interaction of Nanoparticles with Edible Plants and Their Possible Implications in the Food Chain. *J. Agric. Food Chem.* **2011**, *59*, 3485−3498.
(75) Holzworth, G. C. Mixing Depths, Wind Speeds and Air Pollution Potential for Selected Locations in the United States. *J. Appl. Meteorol.* **1967**, *6*, 1039−1044.
(76) Asner, G. P.; Scurlock, J. M. O.; A. Hicke, J. Global Synthesis of Leaf Area Index Observations: Implications for Ecological and Remote Sensing Studies. *Global Ecol. Biogeogr.* **2003**, *12*, 191−205.
(77) Breuer, L.; Eckhardt, K.; Frede, H.-G. Plant Parameter Values for Models in Temperate Climates. *Ecol. Modell.* **2003**, *169*, 237−293.
(78) Hattemer-Frey, H. A.; Travis, C. C. Benzo-a-Pyrene: Environmental Partitioning and Human Exposure. *Toxicol. Ind. Health* **1991**, *7*, 141−157.
(79) Yeo, H.-G.; Choi, M.; Chun, M.-Y.; Sunwoo, Y. Gas/Particle Concentrations and Partitioning of PCBs in the Atmosphere of Korea. *Atmos. Environ.* **2003**, *37*, 3561−3570.
(80) Mackay, D.; Shiu, W. Y. Aqueous Solubility of Polynuclear Aromatic Hydrocarbons. *J. Chem. Eng. Data* **1977**, *22*, 399−402.
(81) Simcik, M. F.; Franz, T. P.; Zhang, H.; Eisenreich, S. J. Gas-Particle Partitioning of PCBs and PAHs in the Chicago Urban and Adjacent Coastal Atmosphere: States of Equilibrium. *Environ. Sci. Technol.* **1998**, *32*, 251−257.
(82) Pirrone, N.; Keeler, G. J.; Holsen, T. M. Dry Deposition of Semivolatile Organic-Compounds to Lake Michigan. *Environ. Sci. Technol.* **1995**, *29*, 2123−2132.
(83) Ryan, P. A.; Cohen, Y. Multimedia Transport of Particle-Bound Organics: Benzo(a)pyrene Test Case. *Chemosphere* **1986**, *15*, 21−47.
(84) Yaffe, D.; Cohen, Y.; Arey, J.; Grosovsky, A. J. Multimedia Analysis of PAHs and Nitro-PAH Daughter Products in the Los Angeles Basin. *Risk Anal.* **2001**, *21*, 275−294.
(85) Harrison, R. M.; Smith, D. J. T.; Luhana, L. Source Apportionment of Atmospheric Polycyclic Aromatic Hydrocarbons Collected from an Urban Location in Birmingham, UK. *Environ. Sci. Technol.* **1996**, *30*, 825−832.
(86) National Climatic Data Center. National Oceanic and Atmospheric Adminstration: 2013.
(87) USCB, *United States Census Bureau QuickFacts*; United States Census Bureau: 2012.
(88) Keller, A. A.; Lazareva, A. Predicted Releases of Engineered Nanomaterials: From Global to Regional to Local. *Environ. Sci. Technol. Lett.* **2014**, *1*, 65−70.
(89) Hendren, C. O.; Mesnard, X.; Dröge, J.; Wiesner, M. R. Estimating Production Data for Five Engineered Nanomaterials As a Basis for Exposure Assessment. *Environ. Sci. Technol.* **2011**, *45*, 2562−2569.
(90) Piccinno, F.; Gottschalk, F.; Seeger, S.; Nowack, B. Industrial Production Quantities and Uses of Ten Engineered Nanomaterials in Europe and the World. *J. Nanopart. Res.* **2012**, *14*, 1−11.
(91) USEPA Water: Sewage Sludge (Biosolids) Frequently Asked Questions. http://water.epa.gov/polwaste/wastewater/treatment/biosolids/genqa.cfm (accessed 10/08/2013).
(92) David, C. A.; Galceran, J.; Rey-Castro, C.; Puy, J.; Companys, E.; Salvador, J.; Monné, J.; Wallace, R.; Vakourov, A. Dissolution Kinetics and Solubility of ZnO Nanoparticles Followed by AGNES. *J. Phys. Chem. C* **2012**, *116*, 11758−11767.
(93) Millero, F. J. Solubility of Fe(III) in Seawater. *Earth Planet. Sci. Lett.* **1998**, *154*, 323−329.
(94) Palmer, D. A.; Bénézeth, P. Solubility of Copper Oxides in Water and Steam. *Proceedings of the 14th Int'l Conf on the Properties of Water and Steam*; 2004; 491−496.
(95) Kent, R. D.; Vikesland, P. J. Controlled Evaluation of Silver Nanoparticle Dissolution Using Atomic Force Microscopy. *Environ. Sci. Technol.* **2011**, *46*, 6977−6984.
(96) Kariuki, S.; Dewald, H. D. Evaluation of Diffusion Coefficients of Metallic Ions in Aqueous Solutions. *Electroanalysis* **1996**, *8*, 307−313.
(97) World Health Organization *Zinc in Drinking-water, Background document for development of WHO Guidelines for Drinking-water Quality*; World Health Organization, Ed.; Geneva, 1996; Vol. *2*.